Radar HRRP Target Recognition with Recurrent Convolutional Neural Networks

Mengqi Shen(✉) and Bo Chen

National Laboratory of Radar Signal Processing, Xidian University, Xian, China
mengqishen_xidian@163.com, bchen@mail.xidian.edu.cn

Abstract. Conventional radar automatic target recognition (RATR) methods using High-Resolution Range Profile (HRRP) sequences require carefully designed feature extraction techniques and plenty of HRRP waveforms, which result in insufficient recognition rate and limit in real-time recognition. To address these issues a modified end-to-end architecture consisting of a convolutional neural network (CNN) followed by a recurrent neural network (RNN) is proposed. In this model the local features of HRRPs extracted by a CNN are passed to a RNN, which avoids manual feature extraction and takes advantage of its shared parameters mechanism which enables single HRRP recognition in real-time. The effectiveness of this model is shown in this paper with numerical results.

Keywords: Radar automatic target recognition (RATR)
High-resolution range profile (HRRP)
Convolutional neural network (CNN)
Recurrent neural network (RNN)

1 Introduction

A high-resolution range profile (HRRP) denotes the coherent summation of projection vectors of complex echoes from target scatters along the radar line-of-sight (LOS). It is a strong function of the target-radar aspect angle and contains abundant informative target structure signatures, e.g. target size, scatters distribution, etc. Compared to a SAR or ISAR image which requires complex preprocessing procedure and substantial amount of calculation [4,17,24,25], an HRRP is easy to obtain, store and process. In recent years, high-resolution radar automatic target recognition (ATR) has received considerable attention.

Several approaches have been proposed to achieve HRR-ATR [4,14,19,20,22,24,34]. These approaches can be roughly divided into two categories according to the treatment of HRRP signatures. One uses single-look HRRP data and the other utilizes multi-look HRRP data. Lots of research [30] indicated that the recognition rate from multi-look HRRP can be higher than that from single-look HRRP because the utilization of multiple of HRRPs brings more information about target, which enlightens us to make use of the multi angle information.

Y. Peng et al. (Eds.): IScIDE 2018, LNCS 11266, pp. 243–251, 2018.
https://doi.org/10.1007/978-3-030-02698-1_21

Previous works about multi-look HRR-ATR mainly include two parts: feature extraction and classifier design [12,23,27]. For example, [9,16,26,33] employed a feature set consisting of the (location, amplitude) pairs of fifteen principal wavefronts selected from the single-look HRR signature by using the RELAX algorithm and fed them to a Hidden Markov Model (HMM) to deal with sequential information. Nevertheless, in these approaches the feature extraction and classifier design are two irrelevant parts which prevent the model automatically from learning the internal representations of the target. Both parts require carefully design and are hard to optimize.

But the development of deep learning has equipped us with different kinds of deep neural networks that are usually designed aiming at specific tasks with an end-to-end manner, which means that the model is trusted to learn the transformations between input and output directly from data. The end-to-end model learns mathematically optimal representations of data without interference by human's knowledge and has achieved state-of-the-art results in plenty of areas. For example, [2] used an end-to-end model to train self-driving cars, [29] provided another novel end-to-end network to generate image captions. In this paper, we utilize an end-to-end architecture consisting of a convolutional neural network (CNN) followed by a recurrent neural network (RNN), which avoids manual feature extraction and enables sequence learning.

It has been convincingly shown that CNNs function well when facing local feature extraction problems due to their shift-invariant attributes [18,28]. As a result they are fit for HRRP recognition because HRRP signatures in the same category share local similarities between sequences. As for RNNs, it passes the extracted sequential features across sequence steps and uses iterative function loops to store temporal information, which enables the learning of time dependencies on multiple scales. Hence we choose CNNs to extract features of single HRRP and then use RNNs to acquire sequential information. In practice this design can be rather useful for that the number of radar echoes reflected from targets of interest are usually uncertain, especially for non-cooperative targets.

There are five sections in the remainder of the paper. Section 2 focuses on a briefly description about CNNs and RNNs. Then we apply the recurrent CNN architecture for HRRP target recognition in Sect. 3. The detailed experiments conducted with the proposed model are provided in Sect. 4. Conclusions come at the end of the paper in Sect. 5.

2 Preliminaries

In this section we will generally review the concepts of convolutional neural network (CNN) and recurrent neural network (RNN).

Convolutional Neural Networks. A CNN is a special case of feedforward neural networks. It consists of one or more convolutional layers, often with a down-sampling layer, which are followed by some fully connected layers in the standard neural network. Each feature map of a convolutional layer receives inputs from a set of features located in a small neighborhood in the previous layer known as local receptive fields.

The convolution operation and weight sharing mechanisms solve "the curse of dimensionality" problem as they reduce the number of parameters, allowing the network to be deeper with fewer parameters. Thus, with deeper layers and different filters CNNs are able to build low level features up to more abstract concepts through a series of convolutional layers.

Recurrent Neural Networks. While some recognition problems can be easily solved by CNNs, there are plenty of temporal data like frames from video, words from sentences which need sequential model to capture their time dependency. Recurrent neural networks utilize the hidden states to pass information across sequence steps, processing sequential data one element at a time. Therefore RNNs can map the entire "history" of previous inputs to each output and take advantage of hidden states to preserve sequential information [21].

A basic RNN is shown in Fig. 1. x denotes an input sequence where each data point x_i is a real-valued vector at time step i. h_i is called a hidden state at time step i which is a non-linear function of the input at the same time step x_i and the hidden state of the previous time step h_{i-1}:

$$h_i = \Phi(Wh_{i-1} + Ux_i). \tag{1}$$

where Φ denotes a non-linear function, and W and U are two different weights matrices. o_i is the output at time step i, which can be calculated by:

$$o_i = \Theta(Vh_i). \tag{2}$$

where Θ is another non-linear mapping function and V is the output weight matrix.

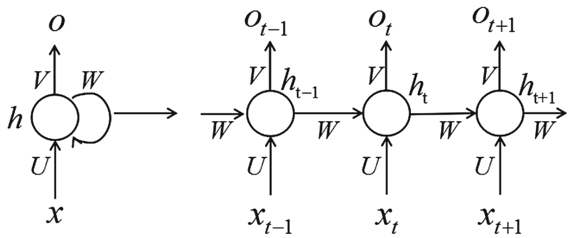

Fig. 1. A basic RNN model in both folded (*left*) and unfolded (*right*) ways

3 Recurrent Convolutional Neural Network for Radar HRRP Target Recognition

Conventional approaches used for radar HRRP target recognition usually ignored the sequential information and depended on carefully designed feature extraction methods. In order to resolve these issues, we apply the Recurrent CNN model in the end-to-end fashion for this recognition problem, which can not only automatically learn the mathematically optimal representation of HRRP data but also make use of multi-aspect HRRP signatures. The architecture of this model is illustrated in Fig. 2.

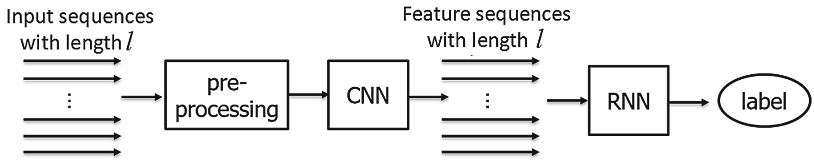

Fig. 2. Our proposed model for HRRP target recognition

3.1 Preprocessing

Before using a CNN for feature extraction, preprocessing procedure for HRRP is conducted due to its complex characteristics about scattering motion through range cells (MTRC) mentioned in [31]. First l_2 normalization is used to normalize the amplitude scale of HRRPs. Then we adopt centroid alignment [1] as a time-shift compensation technique to avoid the relative position shift in HRRP. Figure 3 illustrates examples of preprocessed HRRP data.

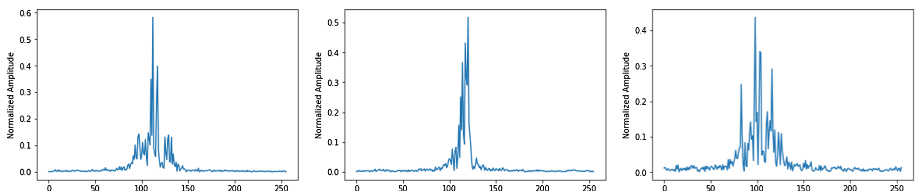

(a) An-26 (b) Cessna Citation S/II (c) Yark-42

Fig. 3. Examples of preprocessed HRRP data in each categories. (a) An-26. (b) Cessna Citation S/II. (c) Yark-42.

3.2 Recurrent CNN Architecture

After preprocessing the normalized and aligned HRRPs are acquired. Let $X_{training} = \{x_1, x_2, ..., x_m\}$ be the training dataset, where x_i is the i-th HRRP data in the training sequence, m is the number of training samples. First we choose a fixed number l, which denotes the number of sequences used in training. l should neither be too large nor too small. Specifically, if l is too large it's difficult for a radar to keep tracking a non-cooperate target so the designed model is not practical. On the contrary if l is too small the model may not use multi-aspect information. At the beginning we simply select $l = 10$ and will discuss the influence of l later in the next section.

During training, a series of HRRP sequences $\{x_1, x_2, ..., x_l\}$ in the same category are input into a multi-layer CNN to obtain feature sequences $\{f_1, f_2, ..., f_l\}$, which are feeded in a followed RNN to predict a label for these successive HRRP signatures. Equations (3)–(5) demonstrate the mathematical details.

$$f_i = H(x_i). \tag{3}$$

$$s_i = \Phi(W f_i + U s_{i-1}). \tag{4}$$

$$label = softmax(\Theta(V s_l)). \tag{5}$$

The non-linear transformation $H(\cdot)$ in CNN can be a composite function of operations such as Batch Normalization (BN) [15], rectified linear units (ReLU) [18], Convolution (Conv) or Pooling [18]. f_i is the feature vector of each HRRP sequence corresponding to x_i. s_i indicates the hidden state at each time step i. Only the last hidden state s_l is used to get a label for these input sequences.

As for testing we apply the well-trained model to recognize single HRRP data in order to achieve real-time recognition. Experiment results are listed in the next section.

4 Experimental Results and Analysis

4.1 Data Description

The results presented in this section are based on measured HRRP data from three real airplanes, which are extensively used in [3,5–8,10,11,31,32]. The basic parameters of the targets and radar are shown in Table 1 and the projections of target trajectories onto the ground plane are shown in Fig. 4.

Table 1. Parameters of planes and radar in the ISAR experiment

Radar parameters	Center frequency	5520 MHz	
	Bandwidth	400 MHz	
Aircraft	Length (m)	Width (m)	Height (m)
Yark-42	36.38	34.88	9.83
Cessna Citation S/II	14.40	15.90	4.57
An-26	23.80	29.20	9.83

When partitioning training datasets and testing datasets there are two things should be taken into account. (1) the training dataset is supposed to cover all possible targets aspect theoretically in order to obtain a well-trained model. (2) the elevation angles of targets in the testing dataset are different from those in the training dataset. Hence we choose the second and the fifth segments of Yark-42, the sixth and the seventh segments of Cessna Citation S/II and the fifth and the sixth segments of An-26 as training samples, and take other data segments as testing samples. All of them are successive in the same segment. The whole training dataset has 140000 HRRP samples and the testing dataset has 7800 HRRP samples in three categories. Each example has 256 range cells, i.e. is a 256-dimensional vector.

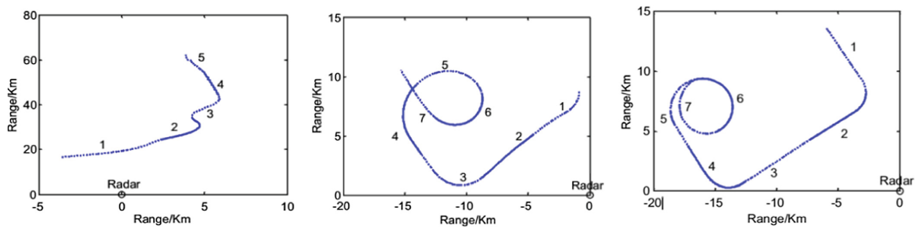

(a) (b) (c)

Fig. 4. Projections of target trajectories onto the ground plane. (a) Yak-42. (b) Cessna Citation S/II. (c) An-26.

4.2 Architectures and Performance

To evaluate the proposed model we have conducted a series of experiments on the dataset described above. In our model, a three-layer CNN with the same size of filters and a RNN with one hidden layer of 16-dimensional LSTM-cells are used [13]. Attempts to optimize the parameters of the model, such as the number of layers and the size of filters in CNN, the dimension of hidden state in LSTM and so on, have been made but these parameters have little effect on the final results. For the output layer the *softmax* activation function which is standard for 1 out of K classification tasks is utilized. The input sequence has a fixed length l. The recognition rates with different l are listed below in Table 2. In order to prove the model's ability and to compare to other methods which also used HRRP sequences to do recognition task. We run some experiments according to [12], whose basic idea is the combination of a feature extraction algorithm and a HMM classifier. The recognition results with the same CNN in our model to extract features and a HMM classifier using l HRRP data is also presented in Table 2. From Table 2 we can tell that recognition rates become better when l increases, which is apparent because the model can use more angular information.

It is necessary to point out that the HMM based model can achieve better result when dealing with Cessna but behave poor in An-26 so the average

Table 2. Summary of obtained results (recognition rate) with CNN-RNN model and CNN-HMM model

Model	$l = 3$	$l = 5$	$l = 8$	$l = 10$	$l = 20$	$l = 30$
CNN + LSTM-RNN	0.925	0.925	0.943	0.947	0.947	0.952
CNN + HMM	0.824	0.845	0.877	0.889	0.890	0.892

recognition rate is far behind the proposed model's. Meanwhile, [23,26,27] all have mentioned a vital procedure, down-sampling, to avoid mutual correlation problem, which requires carefully choosing of sampling rate and weakens the real-time recognition ability. In practice if more than one HRRP signatures can be obtained, the model is also able to utilize the multi-angle information due to its shared parameters. The results in Table 2 show that the recognition accuracy is remarkably improved if successive HRRP sequences are used in the proposed model.

5 Conclusions and Future Work

In this paper, we employ a compact end-to-end Recurrent CNN model for multi-aspect HRRP target recognition task. The model makes use of sequential information on extracted feature of HRRP waveforms and achieves better performance than other sequence model. The contrast experiments using HMM model on the same dataset are also provided. However, the RNN-based model requires same intervals between HRRP sequences and may become infeasible if this condition cannot be guaranteed. In the future we will try to loosen the "time interval" requirement and improve the model's practicability.

References

1. Chen, B., Liu, H.W., Bao, Z.: Analysis of three kinds of classification based on different absolute alignment methods. Mod. Radar **28**(3), 58–62 (2006)
2. Bojarski, M., et al.: End to end learning for self-driving cars (2016)
3. Chen, B., Liu, H., Chai, J., Bao, Z.: Large margin feature weighting method via linear programming. IEEE Trans. Knowl. Data Eng. **21**(10), 1475–1488 (2009)
4. Chiang, H.C., Moses, R.L., Potter, L.C.: Model-based classification of radar images. IEEE Trans. Inf. Theory **46**(5), 1842–1854 (2000)
5. Du, L., Liu, H., Bao, Z., Zhang, J.: Radar automatic target recognition using complex high-resolution range profiles. IET Radar Sonar Navig. **1**(1), 18–26 (2007)
6. Du, L., Liu, H., Bao, Z.: Radar HRRP statistical recognition: parametric model and model selection. IEEE Trans. Signal Process. **56**(5), 1931–1944 (2008)
7. Du, L., Liu, H., Bao, Z., Xing, M.: Radar HRRP target recognition based on higher order spectra. IEEE Trans. Signal Process. **53**(7), 2359–2368 (2005)
8. Du, L., Liu, H., Wang, P., Feng, B., Pan, M., Bao, Z.: Noise robust radar HRRP target recognition based on multitask factor analysis with small training data size. IEEE Trans. Signal Process. **60**(7), 3546–3559 (2012)

9. Du, L., Wang, P., Liu, H., Pan, M., Bao, Z.: Radar HRRP target recognition based on dynamic multi-task hidden markov model. In: Radar Conference, pp. 253–255 (2011)
10. Du, L., Wang, P., Liu, H., Pan, M., Chen, F., Bao, Z.: Bayesian spatiotemporal multitask learning for radar HRRP target recognition. IEEE Trans. Signal Process. **59**(7), 3182–3196 (2011)
11. Feng, B., Du, L., Liu, H.W., Li, F.: Radar HRRP target recognition based on K-SVD algorithm. In: IEEE CIE International Conference on Radar, pp. 642–645 (2012)
12. Fielding, K.H.: Spatiotemporal pattern recognition using hidden markov models. IEEE Trans. Aerosp. Electron. Syst. **31**(4), 1292–1300 (1995)
13. Graves, A.: Long short-term memory. In: Graves, A. (ed.) Supervised Sequence Labelling with Recurrent Neural Networks. SCI, vol. 385, pp. 37–45. Springer, Berlin (2012). https://doi.org/10.1007/978-3-642-24797-2_4
14. Hudson, S., Psaltis, D.: Correlation filters for aircraft identification from radar range profiles. IEEE Trans. Aerosp. Electron. Syst. **29**(3), 741–748 (2002)
15. Ioffe, S., Szegedy, C.: Batch normalization: accelerating deep network training by reducing internal covariate shift, pp. 448–456 (2015)
16. Ji, S., Liao, X., Carin, L.: Adaptive multiaspect target classification and detection with hidden markov models. IEEE Sens. J. **5**(5), 1035–1042 (2005)
17. Jones, G., Bhanu, B.: Recognizing occluded objects in SAR images. IEEE Trans. Aerosp. Electron. Syst. **37**(1), 316–328 (2001)
18. Krizhevsky, A., Sutskever, I, Hinton, G.E.: ImageNet classification with deep convolutional neural networks. In: International Conference on Neural Information Processing Systems, pp. 1097–1105 (2012)
19. Li, H.J., Yang, S.H.: Using range profiles as feature vectors to identify aerospace objects. IEEE Trans. Antennas Propag. **41**(3), 261–268 (1993)
20. Liao, X., Bao, Z., Xing, M.: On the aspect sensitivity of high resolution range profiles and its reduction methods. In: The Record of the IEEE 2000 International Radar Conference, pp. 310–315 (2000)
21. Mikolov, T., Karafit, M., Burget, L., Cernocky, J., Khudanpur, S.: Recurrent neural network based language model. In: INTERSPEECH 2010, Conference of the International Speech Communication Association, Makuhari, Chiba, Japan, September, pp. 1045–1048 (2010)
22. Mitchell, R.A., Westerkamp, J.J.: Robust statistical feature based aircraft identification. IEEE Trans. Aerosp. Electron. Syst. **35**(3), 1077–1094 (1999)
23. Nilubol, C., Pham, Q.H., Mersereau, R.M., Smith, M.J.T., Clements, M.A.: Hidden markov modelling for SAR automatic target recognition. In: IEEE International Conference on Acoustics, Speech and Signal Processing, vol. 2, pp. 1061–1064 (1998)
24. Novak, L.M.: State-of-the-art of SAR automatic target recognition. In: The Record of the IEEE 2000 International Radar Conference, pp. 836–843 (2000)
25. O'Sullivan, J.A., Devore, M.D., Kedia, V., Miller, M.I.: SAR ATR performance using a conditionally Gaussian model. IEEE Trans. Aerosp. Electron. Syst. **37**(1), 91–108 (2001)
26. Pei, B., Bao, Z.: Multi-aspect radar target recognition method based on scattering centers and HMMs classifiers. Acta Electronica Sinica **41**(3), 1067–1074 (2003)
27. Runkle, P., Nguyen, L.H., Mcclellan, J.H., Carin, L.: Multi-aspect target detection for SAR imagery using hidden markov models. IEEE Trans. Geosci. Remote. Sens. **39**(1), 46–55 (2001)

28. Szegedy, C., et al. Going deeper with convolutions. In: IEEE Conference on Computer Vision and Pattern Recognition, pp. 1–9 (2015)
29. Vinyals, O., Toshev, A, Bengio, S., Erhan, D.: Show and tell: a neural image caption generator, pp. 3156–3164 (2014)
30. Williams, R., Westerkamp, J., Gross, D., Palomino, A.: Automatic target recognition of time critical moving targets using 1D high range resolution (HRR) radar. IEEE Aerosp. Electron. Syst. Mag. **15**(4), 37–43 (2000)
31. Xing, M., Bao, Z., Pei, B.: Properties of high-resolution range profiles. Opt. Eng. **41**(2), 493–504 (2002)
32. Da Zhang, X., Shi, Y., Bao, Z.: A new feature vector using selected bispectra for signal classification with application in radar target recognition. IEEE Trans. Signal Process. **49**(9), 1875–1885 (2001)
33. Zhu, F., Da Zhang, X., Hu, Y.F., Xie, D.: Nonstationary hidden Markov models for multiaspect discriminative feature extraction from radar targets. IEEE Trans. Signal Process. **55**(5), 2203–2214 (2007)
34. Zyweck, A., Bogner, R.E.: Radar target classification of commercial aircraft. IEEE Trans. Aerosp. Electron. Syst. **32**(2), 598–606 (1996)